



Fault Ride-Through Improvement of an Offshore DFIG Wind Turbine

Kouider Khaled^(✉) and Bekri Abdelkader

Department of Electrical Engineering, University of Tahri Mohammed,
Bechar, Algeria

khouiledkhaled@gmail.com, bekriabdkader@yahoo.fr

Abstract. Fault ride through (FRT) is recognized as one of the most exciting topics in inspecting wind turbine performance. In this paper, the behavior of a DFIG offshore wind farm under fault circumstances is reviewed. Three case studies basing on the 3-phase fault location are taken into account. In this situation, the crowbar protection is primordial to prevent any over-currents in the rotor windings and to short the Rotor side converter (RSC) from the system. However, the use of this protection individually is insufficient and causes a lack of rotor speed and reactive power control. Here, the need for the internal model control (IMC) for the grid side converter (GSC) is essential to intensify the fault ride through capabilities of the DFIG. The simulation is performed using MATLAB/SIMULINK. As the results show, the use of the IMC for the grid side converter with the crowbar protection boosts both the Fault ride through and the performance of the DFIG.

Keywords: Grid side converter (GSC) · Rotor side converter (RSC) · Doubly fed induction generator (DFIG) · Internal model control (IMC) · Wind turbine · Fault ride through (FRT)

1 Introduction

Day after day, renewable energies do not stop growing and breaking new records in the global energy markets. Several factors push up the world to find new clean and harmless energy sources. Due to its significant potential in the energy markets, wind energy is considered one of the most relevant renewable sources [1]. The last statistics from [2] proves that wind energy leads all the other renewable energies with a more than 590 MW as the total capacity and a new installed capacity of 51.3 MW only in 2018 (46.3 MW onshore, 4.5 offshore). The DFIG was introduced to the wind power generation system due to many advantages, such as economic benefits, the partial scale conversion, lightweight mechanism structure, and many other factors. The grid is suddenly affected by many tips of disturbances, such as faults, voltage dips, and so on, and since the DFIG is directly connected to the grid via its stator. Thus, this machine will be susceptible to these abrupt circumstances. For the grid code requirements, the DFIG should support these fault conditions and remain connected to the grid, which is known as the fault ride through (FRT). Because of a large wind farm of 315 MW disconnection and leads to a non-fault ride through, Australia was suffered from a

Blackout on 28 September 2016 [3]. The crowbar protection is a crucial part to preserve the Rotor side converter (RSC) and to ensure the fault ride through obligation as well [3].

Many kinds of research are carried out about the fault ride through (FRT), a crowbar protection system application to A DFIG wind system is well discussed in [4], Enhanced Fault Ride-Through Ability of DFIG using Superconducting Fault Current Limiter [5], a nonlinear dynamic modeling for fault ride-through capability of DFIG-based wind farm is performed by [6]. The detailed configuration and control laws are well examined and established in various works such as [7–9]. In this paper, the crowbar protection will be employed for the RSC converter to ensure high protection against large rotor currents overshoots. The whole system used in this paper is well displayed in Fig. 1. To ensure high performance and robust response against these faults, the Internal Model Control (IMC) is used for the Grid side converter (GSC). Eventually, this paper will be divided into three main parts: 1-mathematical modeling of the wind system, 2-The overall control of the Back-to-Back converter, 3-Simulation results and discussion.

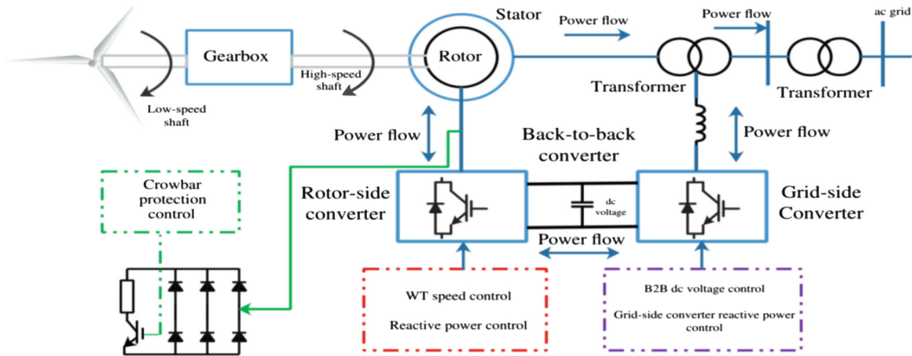


Fig. 1. DFIG wind turbine system with crowbar protection.

2 DFIG Wind System Modeling

In this section, the mathematical modeling of the overall DFIG wind system will be examined.

2.1 DFIG Mathematical Modeling

Basing on the dq synchronous reference frame, the analytical model of the machine can be re-written employing the stator and rotor windings equations as follows:

$$\begin{aligned}
u_{sd} &= R_s i_{sd} + \frac{d\psi_{sd}}{dt} - \omega_s \psi_{sq} \\
u_{sq} &= R_s i_{sq} + \frac{d\psi_{sq}}{dt} + \omega_s \psi_{sd} \\
u_{rd} &= R_r i_{rd} + \frac{d\psi_{rd}}{dt} - \omega_r \psi_{rq} \\
u_{rq} &= R_r i_{rq} + \frac{d\psi_{rq}}{dt} + \omega_r \psi_{rd}
\end{aligned} \tag{1}$$

After that, the Eq. (2) represents the stator and rotor flux with L_m, L_s, L_r are the mutual, stator and rotor inductances:

$$\begin{aligned}
\psi_{sd} &= L_s i_{sd} + L_m i_{rd} \\
\psi_{sq} &= L_s i_{sq} + L_m i_{rq} \\
\psi_{rd} &= L_r i_{rd} + L_m i_{sd} \\
\psi_{rq} &= L_r i_{rq} + L_m i_{sq}
\end{aligned} \tag{2}$$

Moreover, the electromagnetic torque:

$$T_{em} = \frac{3}{2} p (i_{rd} i_{sq} + i_{rq} i_{sd}) \tag{3}$$

3 Back-to-Back (B2B) Modeling and Control

One of the most dominant interfaces in wind power application is the Back-to-Back (B2B) converter. The topology of this Voltage Source Converter (VSC) is well discussed and detailed in several references like [7, 8], [10, 11]. As shown in the Fig. 1, this converter consists of two Voltage Sources converters, one for the machine (Rotor Side converter) (RSC), and the other is the grid side converter (GSC). To ensure high performance and accurate control of the DFIG wind system, this converter should be commanded appropriately. In the next subsections, both vector control strategies for the two converters will be concisely reviewed.

3.1 RSC Control

The primary role of the rotor side converter is to adjust both rotor speed and stator reactive power. In a DFIG wind system, the stator active and reactive power can be commanded independently using suitable rotor currents injections. Basing on the dq synchronous reference frame, and corresponding to the comprehensive development of the classic vector control method for the RSC converter in [7], we can see that I_{dr} control the torque, while the reactive power is directly affected by I_{qr} .

$$T_e = -\frac{3}{2}p \left(\frac{-L_m \psi_{qs}}{L_m + L_{ls}} \right) i'_{dr} \tag{4}$$

$$Q_s = \frac{3}{2} \left[v_{ds} \left(\frac{\psi_{qs} - L_m i'_{dr}}{L_{ls} + L_m} \right) \right] \tag{5}$$

3.2 GSC Control

The grid side converter GSC is the second part of the back-to-back converter which links the DFIG with the grid. Many types of research are examining the vector control strategies for the GSC of the DFIG like in [9], [12–14]. In this paper, we will use the Internal Model Control as an additional controller for the GSC controller to enhance the fault ride through and to ensure high grid voltage and currents control. In this paper, we will use the Internal Model Control as an additional controller for the GSC controller to enhance the fault ride through and to establish high grid voltage and currents control.

The 2-degree of freedom IMC controller applied in this paper is well described in [7], the final development of the system equation of this controller yields:

$$M_{gsc}(s) = \frac{1}{G_{gsc} + L_s + r} \tag{6}$$

$$v_{gsc}(s) = v'_{gsc}(s) - i_{gsc}(s)G_{gsc} \tag{7}$$

$$F_{gsc}(s) = \alpha_{gsc}L + \frac{(r + G_{gsc})\alpha_{gsc}}{s} \tag{8}$$

$$Kp_{gsc} = \alpha_{gsc}L \text{ and } Ki_{gsc} = (r + G_{gsc})\alpha_{gsc}$$

α_{gsc} is the bandwidth of the closed loop system of i_{gsc} .

Then, the two-degree-of-freedom GSC currents IMC control loop is well presented in Fig. 2.

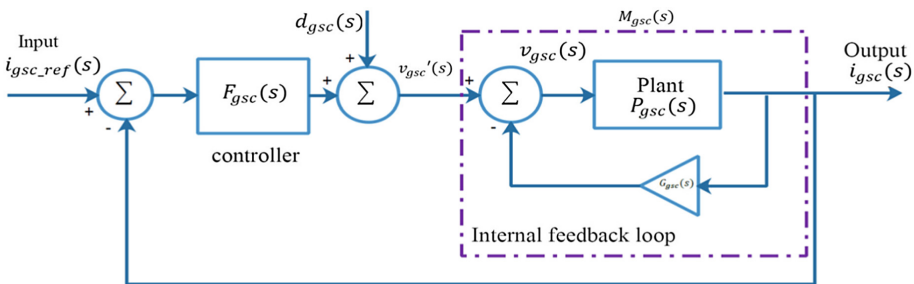


Fig. 2. Two degree-of-freedom for GSC currents IMC control loop.

Finally, the complete GSC converter control including the IMC controller is exposed in Fig. 3. The MATLAB/SIMULINK model of the GSC with the IMC is well described in the appendix in the associated Supplementary Material.

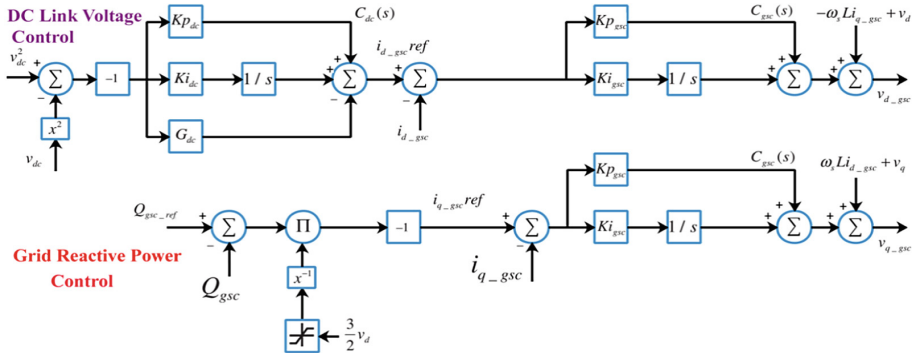


Fig. 3. Configuration diagram of GSC controllers.

4 Results and Discussion

The simulation was implemented using the MATLAB/SIMULINK Software Package. To investigate the behavior of an offshore DFIG wind farm under fault conditions, we take three case studies into account, as indicated in Fig. 4. All the data handled in the simulation are mentioned in the Appendix included in the (Supplementary Material). To study the performance of the applied Internal Model Control (IMC) control for the grid side converter (GSC), a three phases-fault is tested at 8 s and cleared after 85 ms in each case. Before that, the DFIG can generate 0.71 pu of active power with a wind speed of 11 m/s.

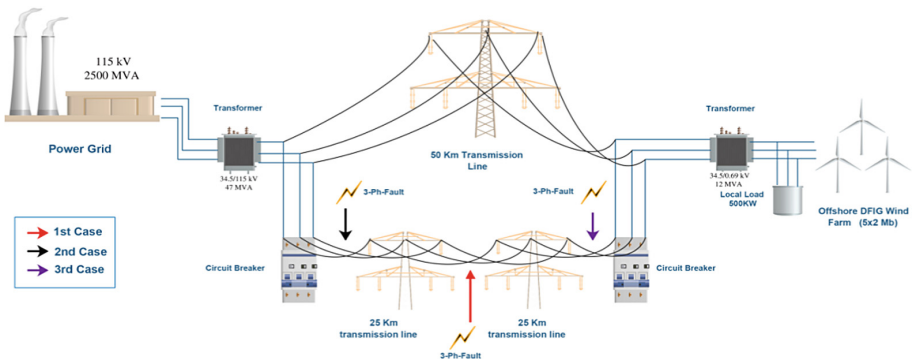


Fig. 4. The overall diagram of the simulation case studies.

The Figs. 5, 6, 7, 8 and 9 show all the most important electrical parameters of the DFIG such rotor voltages and currents, DC link voltage, stator active and reactive power, and finally the on/off crowbar trigger function.

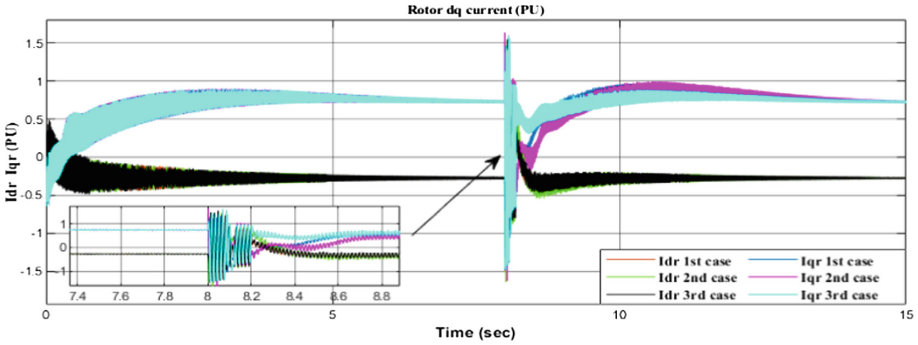


Fig. 5. The dq components of the rotor current.

The Fig. 5 shows the dq components of rotor current. In case 1 and 2 the magnitude of I_r still less than the crowbar triggering current and the turbine remains connected, while in case 3 the magnitude rise above the I_{crow} causing that the crowbar protection intervention and disconnect the turbine from the grid.

As demonstrated in Fig. 6, the rotor voltage has a massive augmentation in amplitude just after the fault application. In addition to that, in the three cases, we can see that the system is suffering from two interruptions (8.054 s–8.075 s) and from (8.11 s–8.17 s), inducing a lack of RSC control. After fault clearance, the rotor voltage regains gradually.

The Fig. 7 shows the active and reactive power driven from the stator. Obviously, the reactive power is well controlled near to 0 pu, when the active power approaches

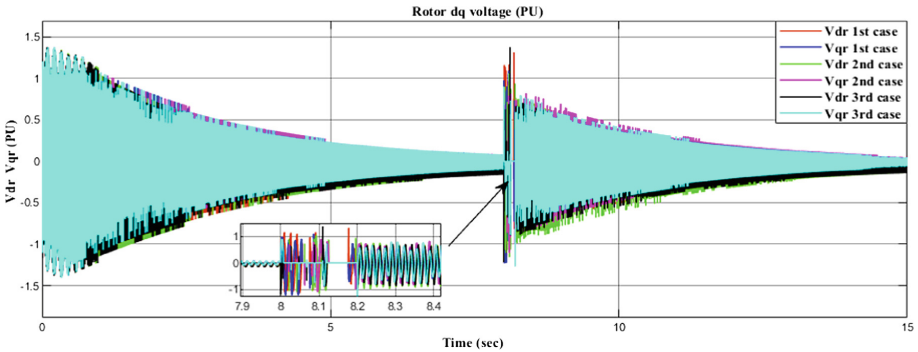


Fig. 6. The dq components of the rotor voltage.

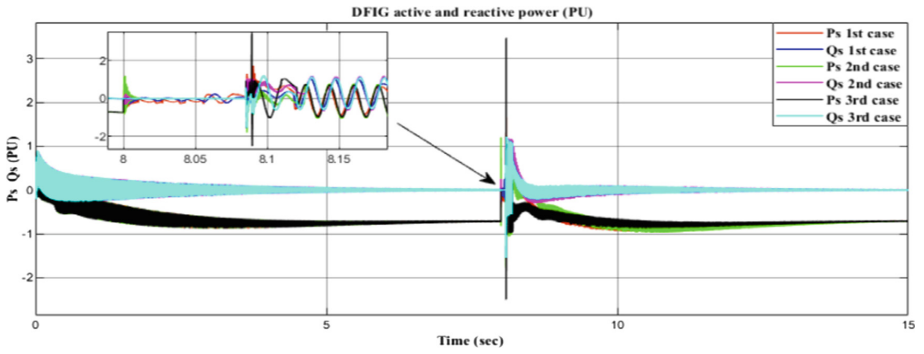


Fig. 7. Active and reactive power delivered from the stator.

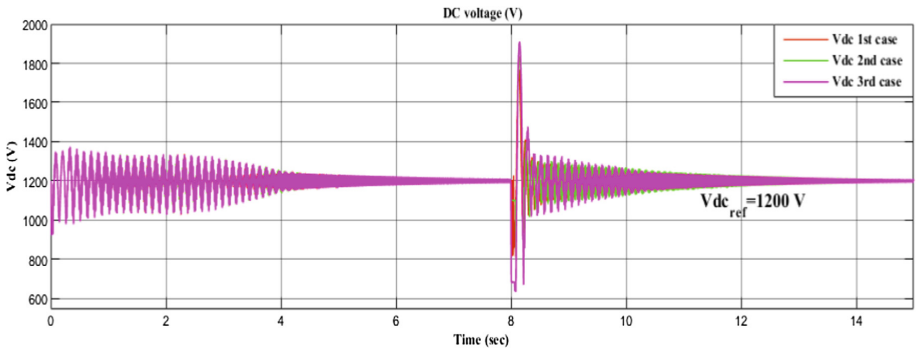


Fig. 8. The DC link voltage evolution.

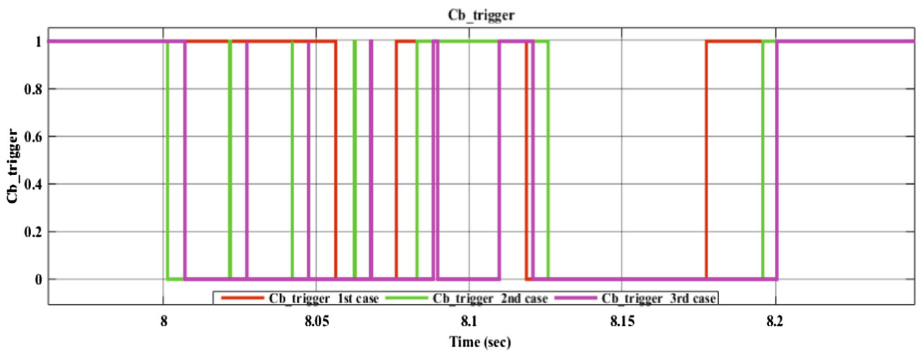


Fig. 9. The crowbar trigger function.

0.71 pu in the pre-fault. When the fault is applied, we can observe that there is a loss in power control because of the interruptions in the rotor voltage. After the fault, both P_s and Q_s restore their rated values rapidly.

Eventually, Fig. 8 establishes the DC link voltage. When the crowbar protection acts ($V_{dc} > V_{crowb}$) or ($I_r > I_{crow}$), the DC link voltage starts discharging, and after the fault clearance, the GSC maintains the dc link voltage to its reference value. While the Fig. 9 shows the trigger function of the crowbar in the three cases. We can figure out that, the crowbar protection is activated when using the logic comparator with the pre-set Dc voltage and rotor current to prevent any damage for the RSC.

5 Conclusion

In this work, a dynamic model of a grid-connected DFIG together with crowbar protection is achieved. After that, we briefly review the complete vector control of both RSC and GSC including the IMC control technique in Sect. 2. In the last part, the simulation of the three cases based on the fault location is performed. Basing on the simulation results, we can conclude that the fault ride through of the tested wind farm is highly affected by the 3-phase fault location. Also, since the FRT is a high necessity, the associated controllers must be well exploited, and their parameters must precisely be chosen. Finally, the results showed that the crowbar protection is not enough and must be accompanied by the IMC controller to help the machine to ride through the fault or at least, to reduce any severe currents fastly.

References

1. Global Wind Energy Council (GWEC): Global Wind Report—Annual Market Update; Global Wind Energy, Council (GWEC), Brussels, Belgium, p. 61, April 2019
2. Duong, M.Q., Leva, S., Mussetta, M., Le, K.H.: A comparative study on controllers for improving transient stability of DFIG wind turbines during large disturbances. *Energies* **11** (3), 480 (2018)
3. Romphochai, S., Pichetjamroen, A., Teerakawanich, N., Hongesombut, K. (eds.): Coordinate operation of fuzzy logic voltage regulator and Bi-2212 SFCL for enhancing fault ride through capability of DFIG wind turbines. In: 2017 International Electrical Engineering Congress (iEECON), pp. 1–4 (2017)
4. Salles, M.B.C., Hameyer, K., Cardoso, J.R., Grilo, A.P., Rahmann, C.: Crowbar system in doubly fed induction wind generators. *Energies* **3**(4), 738–753 (2010)
5. Sahoo, S., Mishra, A., Chatterjee, K., Sharma, C.K. (eds.): Enhanced fault ride—Through ability of DFIG-based wind energy system using superconducting fault current limiter. In: 2017 4th International Conference on Power, Control & Embedded Systems (ICPCES), pp. 1–5 (2017)
6. Döşoğlu, M.K.: Nonlinear dynamic modeling for fault ride-through capability of DFIG-based wind farm. *Nonlinear Dyn.* **89**(4), 2683–2694 (2017)
7. Anaya-Lara, O., Campos-Gaona, D., Moreno-Goytia, E., Adam, G.: Offshore Wind Energy Generation Control, Protection, and Integration to Electrical Systems, p. 307. Wiley, Hoboken (2014)

8. Abu-Rub, H., Malinowski, M., Al-Haddad, K.: *Power Electronics for Renewable Energy Systems, Transportation and Industrial Applications*, p. 827 (2014)
9. Abad Jsp, G., Rodriguez, M.A., Marroyo, L., Iwanski, G.: *Power Electronics and Electric Drives for Traction Applications*, p. 684. Wiley, Hoboken (2016)
10. Teodorescu, R., Liserre, M., Rodriguez, P.: *Grid Converters for Photovoltaic and Wind Power Systems*, p. 407. Wiley, Hoboken (2011)
11. Wu, B., Lang, Y., Zargari, N., Kouro, S.: *Power Conversion and Control of Wind Energy System*, p. 480. Wiley, Hoboken (2011)
12. Kerrouche, K., Mezouar, A., Belgacem, K.: Decoupled control of doubly fed induction generator by vector control for wind energy conversion system. *Energy Procedia* **42**, 239–248 (2013)
13. Chowdhury, M.A., Hijazin, I., Hosseinzadeh, N., Pota, H.R.: *Modeling-and-Analysis-With-Induction-Generators*. CRC Press, p. 486 (2015)
14. Ali, M.H.: *Wind Energy Systems; Solutions for Power Quality and Stabilization*, p. 287. CRC Press, Boca Raton (2012)